Landscape Ecology **19:** 197–209, 2004.

Research article

Effects of remote sensor spatial resolution and data aggregation on selected fragmentation indices

Santiago Saura
Department of Agroforestry Engineering, Higher Technical School of Agrarian Engineering, University of Lleida, Av. Alcalde Rovira Roure, 191, 25198, Lleida, Spain; (e-mail: ssaura@eagrof.udl.es)

Received 18 July 2002; accepted in revised form 15 September 2003

Key words: Fragmentation index, Grain, Landscape pattern, Pixel size, Power law, Pattern aggregation, Scale, Spatial configuration, Spatial resolution

Abstract

Analyzing the effect of scale on landscape pattern indices has been a key research topic in landscape ecology. The lack of comparability of fragmentation indices across spatial resolutions seriously limits their usefulness while multi-scale remotely sensed data are becoming increasingly available. In this paper, we examine the effect of spatial resolution on six common fragmentation indices that are being used within the Third Spanish National Forest Inventory. We analyse categorical data derived from simultaneously gathered Landsat-TM and IRS-WiFS satellite images, as well as TM patterns aggregated to coarser resolutions through majority rules. In general, majority rules tend to produce more fragmented patterns than actual sensor ones. It is suggested that sensor point spread function should be specifically considered to improve comparability among satellite images of varying pixel sizes. Power scaling-laws were found between spatial resolution and several fragmentation indices, with mean prediction errors under 10% for number of patches and mean patch size and under 5% for edge length. All metrics but patch cohesion indicate lower fragmentation at coarser spatial resolutions. In fact, an arbitrarily large value of patch cohesion can be obtained by resampling the pattern to smaller pixel sizes. An explanation and simple solution for correcting this undesired behaviour is provided. Landscape division and largest patch index were found to be the least sensitive indices to spatial resolution effects.

Introduction

Quantification of landscape fragmentation through pattern indices is currently a common practice in landscape ecology and related disciplines. These indices capture some of the spatial characteristics that have been found relevant for different ecological or physical processes (e.g., Forman 1995). In particular, fragmentation indices derived from remotely sensed data are being increasingly used for landscape assessment and land cover change characterization (Luque et al. 1994; Sachs et al. 1998; Chuvieco 1999; Griffiths et al. 2000; Luque 2000; Hansen et al. 2001; Imbernon and Branthomme 2001). Satellite images are used as the primary source of spatial information because they provide the digital mosaic of landcovers convenient for the computation of these indices (Chuvieco 1999). At the same time, the development of remote sensing and GIS has made available a wide variety of spatial data. It is now possible to compare and integrate landscape data at different scales.

Many studies have provided insights into the effect of spatial resolution on landscape indices (Turner et al. 1989a; Benson and MacKenzie 1995; Wickham and Riitters 1995; Frohn 1998; Wu et al. 2000; Wu et al. 2002), which is related to the more general modifiable areal unit problem (e.g., Openshaw 1984; Jelinski and Wu 1996). However, only the study by Benson and MacKenzie (1995) directly compared fragmentation indices computed on simultaneously

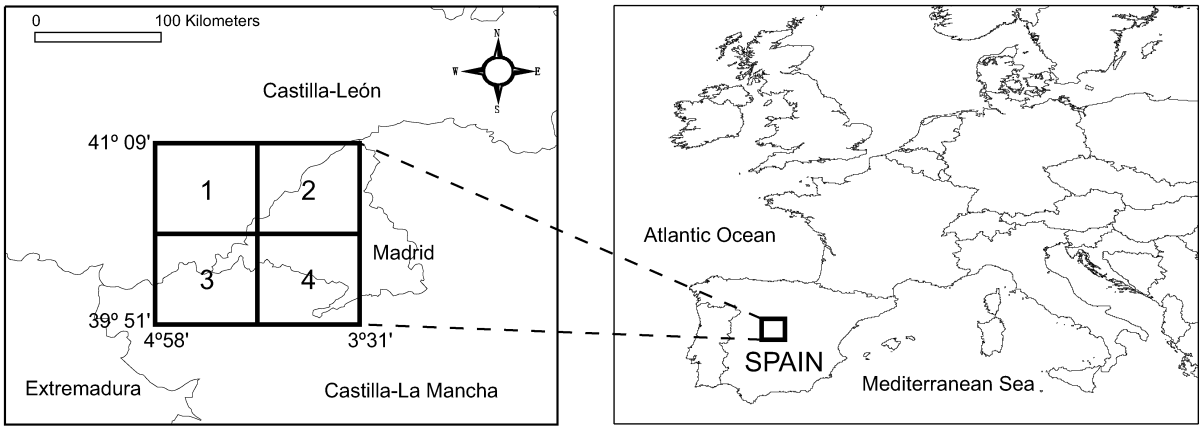

Figure 1. Location of the study area and the four zones in which the overlapping area between Landsat-TM and IRS-WiFS scenes was divided.

gathered satellite images with different spatial resolutions for the same landscape. Also, some recently introduced indices (Schumaker 1996; Jaeger 2000) have not been analyzed in previous studies. Although it is well-known that there are large differences in the values of the fragmentation indices derived from satellite images with different spatial resolutions, it is not yet fully understood how fragmentation indices are affected by spatial resolution. For the practical use of fragmentation indices it is generally recommended not comparing the values of the indices when they have been measured at different spatial resolutions (e.g., Turner et al. 1989b; McGarigal and Marks 1995). Further studies are needed, because the lack of comparability across scales seriously limits the potential usefulness of quantitative analysis of landscape patterns.

This study analyzes the effect of spatial resolution on several common indices that are being used to characterise forest fragmentation within the Third Spanish National Forest Inventory (Ministerio de Medio Ambiente 2002). We intend to provide further insights into the following questions: how do these fragmentation indices behave with varying sensor spatial resolutions? Which fragmentation indices can be directly compared across spatial resolutions? When not, is it possible to correct their behaviour in order to render comparable multi-scale fragmentation estimates?

Data and methods

Spatial data

There are two main approaches to generate categorical spatial patterns with different spatial resolutions for a given landscape. The more common and simpler one is spatial aggregation. Majority rules have been commonly used for this purpose in landscape ecology (Turner et al. 1989a; Benson and MacKenzie 1995; Wickham and Riitters 1995; Frohn 1998; Wu et al. 2002). These studies assumed that majority rules could produce aggregated patterns adequately similar to those directly mapped through remote sensors with coarser spatial resolutions. The other approach is directly classifying simultaneously gathered satellite images covering the same study area but with different sensor spatial resolutions. This latter approach has been less commonly used in landscape ecological studies (but see Benson and MacKenzie 1995).

This study considered both approaches. The aggregation approach allowed us to easily generate spatial data covering a wide range of spatial resolutions. Coetaneous satellite data were used to validate some of the results obtained with aggregated data. They also allowed for comparison of the patterns produced by majority rules with those derived from coarser spatial resolution satellites.

Landsat-TM and IRS-WiFS patterns

We selected two simultaneously gathered scenes covering the same area in central Spain (Figure 1) from satellite sensors with different spatial resolutions: a

Landsat Thematic Mapper (TM) scene (30 meter resolution) acquired on the 29th September 1999 at 10:32, and a IRS-1D-WiFS (Wide Field Sensor on board the Indian Remote Sensing Satellite 1D) scene acquired the same day at 11:33. Although the nominal spatial resolution of the IRS-WiFS sensor is 188 m (NRSA 1995), the WiFS image was available as a path-oriented data product resampled to 180 m (the nearest neighbour method). WiFS scene was registrated to Landsat-TM with sub-pixel accuracy. The full overlapping area was divided in four zones (Figure 1), each covering 2,000 × 2,000 pixels in the Landsat-TM data (360,000 ha), for subsequent cross-zone comparison.

Both sensors have red (R) and near infrared (NIR) spectral bands (e.g., Chuvieco 2002), from which we computed the NDVI (normalized difference vegetation index) from the digital signal levels of the images:

$$NDVI = \frac{NIR - R}{NIR + R} \quad (1)$$

NDVI has several characteristics suited for the discrimination of vegetation patterns: it reduces the effect of slope and orientation in vegetation spectral response, and positively correlates with forest canopy cover, leaf area index, vegetation moisture and productivity (e.g., Myneni et al. 1995; Chuvieco 2002).

From the NDVI we generated several categorical images for each zone and sensor. We selected threshold values of the NDVI that classified the landscape in two types: low-NDVI areas (class 1, sparse and/or dry vegetation) and high NDVI areas (class 2, abundant and/or vigorous vegetation). The threshold values (different for TM and WiFS data) were selected so that the high-NDVI class abundance (percent of total area occupied by that class) was varied for each sensor from 10% to 90% (± 1%) with interval 10%. In total, we obtained 36 binary images for each of the two sensors (9 for each of the four zones). This simple classification method allows obtaining a wide range of class abundances. This is important because class abundance has been shown to significantly influence the values and scaling behaviour of landscape indices (e.g., Saura and Martínez-Millán 2001).

It should be noted that some differences exist in the red (R) and near infrared (NIR) bands for the WiFS and TM sensors, and this has been shown to have some impact on the resultant NDVI values (Teillet et al. 1997). The wavelengths of WiFS bands are 620-680 nm (R) and 770-860 nm (NIR) while those of TM are 630-690 nm and 760-900 nm (e.g., Chuvieco 2002). The width of the red band is the same for both sensors, but NIR band is much wider on the TM sensor. There are also slight differences on the center wavelengths for each band, but these differences tend to have opposite effects on NDVI values (Teillet et al. 1997). That is, wider NIR bands tend to produce lower NDVI values, while higher center wavelengths for NIR bands implicate higher NDVI values. As a result of these effects only small differences are expected between the NDVI obtained from TM and WiFS sensors (an absolute difference smaller than 0.02 according to the results presented by Teillet et al. (1997)). Moreover, the differences tend to be similar among the different vegetation types analyzed by Teillet et al. (1997). Thus, the same vegetation types are those with the highest (and lowest) NDVI values both in TM and WiFS data. This is the only assumption required to generate equivalent categorical datasets for both sensors according to the NDVI-threshold procedure.

Majority rules and Landsat-TM patterns

We applied majority rules to coarsen the spatial resolution of the 36 categorical images derived from the Landsat-TM scene. Majority rules assign to the degraded image the most frequent class in windows of $F \times F$ pixels, where F is the aggregation factor or the relation between the length of a pixel in the degraded and original image. Categorical patterns were degraded to eight additional spatial resolutions corresponding to the aggregation factors $F=2$, 3, 4, 5, 6, 10, 30 and 50 pixels. An example of the resultant patterns for $F=6$ is shown in Figure 2.

Fragmentation indices

We examined six indices that are being used to characterise forest fragmentation within the Third Spanish National Forest Inventory (Ministerio de Medio Ambiente 2002). We adopt a broad definition of fragmentation that includes the combined effects of habitat loss and breaking of habitats (e.g., Andrén 1994; Schumaker 1996; Jaeger 2000). Number of patches, mean patch size, edge length and largest patch index have been widely used for landscape pattern analysis (e.g., Iverson 1988; Turner and Ruscher 1988; Forman 1995; Griffiths et al. 2000; Tischendorf

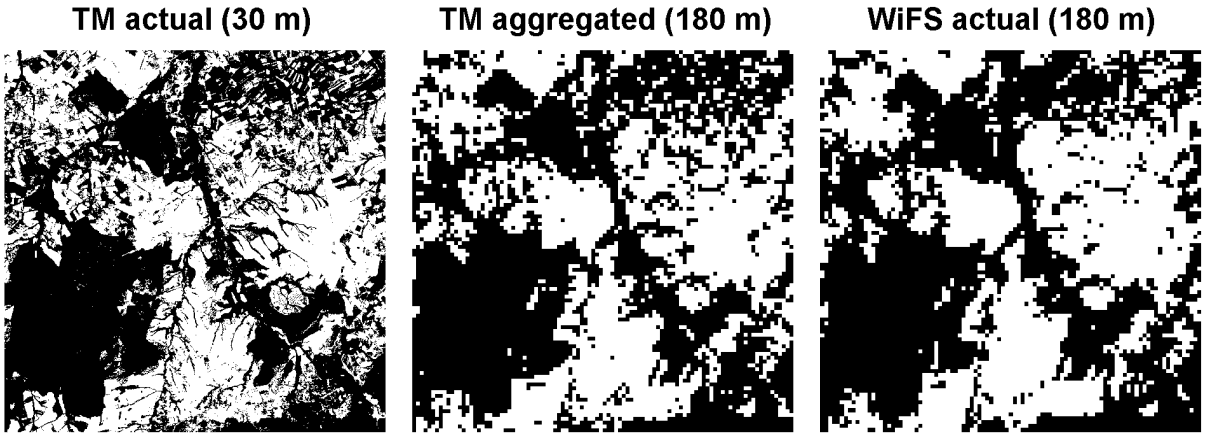

Figure 2. Comparison of actual TM and WiFS patterns and TM patterns aggregated to WiFS resolution through majority rules. The three images correspond to the same subset within the study area. The spatial resolution of each image is indicated between brackets.

2001). Patch cohesion (Schumaker 1996) and landscape division (Jaeger 2000) have been more recently introduced and present potential improvements over existing indices. All the fragmentation indices were computed at the class level (i.e., considering only those patches belonging to a certain class) using C++ programs. The six fragmentation indices are:

(1) Number of patches (NP). A patch is defined here by the 4-neigborhood rule. NP can be used as a fragmentation index (e.g., Turner and Ruscher 1988), with higher NP indicating greater fragmentation.

(2) Mean patch size (MPS). This is a simple and common fragmentation index (e.g., Turner and Ruscher 1988), with lower MPS indicating greater fragmentation:

$$MPS = \frac{\sum_{i=1}^{NP} a_i}{NP} \tag{2}$$

where a_i is the area of each of the NP patches of the land cover class of interest.

(3) Edge length (EL). An edge is defined as the length of any side shared between two pixels belonging to different classes. EL is regarded as a good indicator of pattern fragmentation (Li et al. 1993), with more fragmented landscapes yielding higher EL. Edges defined by the map border are not included in EL.

(4) Largest patch index (LPI). LPI is the percent of total landscape area occupied by the largest size patch of the class of interest (McGarigal and Marks 1995).

(5) Landscape division (LD). LD is defined as the probability that two randomly chosen places in the landscape are not situated in the same patch of the class of interest (Jaeger 2000). So, higher LD values indicate increased fragmentation. It is computed as:

$$LD = 1 - \sum_{i=1}^{NP} \left[\frac{a_i}{A_T} \right]^2 \tag{3}$$

where A_T is total landscape area. Large patches contribute to the decrease of the total probability in a greater proportion than smaller ones, as indicated by the squared terms in Equation (3). In particular, if the largest patch occupies a high percentage of total class area, the contribution of the rest of the patches to Equation (3) becomes minor. For this reason, LD may be highly correlated with LPI. So are effective mesh size and splitting index, which can be computed directly from LD (Jaeger 2000).

(6) Patch cohesion (PC) index. PC is given by:

$$PC = \left[1 - \frac{\sum_{i=1}^{NP} p_i}{\sum_{i=1}^{NP} p_i \cdot \sqrt{a_i}} \right] \cdot \left[1 - \frac{1}{\sqrt{N}} \right]^{-1} \tag{4}$$

where p_i and a_i are, respectively, the perimeter and the area of each of the NP patches of the class of interest, and N is the total number of pixels in the landscape. a_i and p_i are expressed respectively as the number of pixels and pixel edges of a patch (Schumaker 1996).

This way, when all patches of habitat are confined to single isolated pixels PC attains its minimum value (PC=0), while PC reaches the maximum (PC=1) when a single habitat patch fills the whole landscape. Higher PC values indicate lower fragmentation. Schumaker (1996) found that PC was better linearly correlated with animal populations dispersal success than other commonly used landscape indices. Tischendorf (2001) partially supported this result.

We can quantify the mean sensitivity to spatial resolution of the indices in the whole data set (*SM*) with the following expression (O'Neill et al. 1996; Saura and Martínez-Millán 2001; Saura 2002):

$$S_M = 100 \cdot \frac{\sum_{i=1}^{n} \left| I_i^{180} - I_i^{30} \right|}{n \cdot SD} \qquad (5)$$

where I^{30} and I^{180} are respectively the values of the fragmentation index at spatial resolutions of 30 meters (Landsat-TM) and 180 meters (Landsat-TM degraded to IRS-WiFS resolution through majority rules, $F=6$). In our analysis, $n=72$ (two NDVI-classes, four zones, and nine different values of class abundance). *SD* is the standard deviation of the index in the full set of Landsat-TM patterns, indicating the different range of variation of each index.

Results

Comparison of aggregated and actual sensor patterns

We found considerable differences between the indices values of the actual WiFS data and those of TM data aggregated through majority rules (Table 1). Benson and MacKenzie (1995) concluded that extrapolated indices values using majority rules closely approximated the actual sensor values. However, this is not the case for all fragmentation indices in our study. NP, MPS and EL indicate that majority rules produced clearly more fragmented patterns than actual sensor ones for the four zones (Table 1). The rest of the fragmentation indices did not show a systematic difference between the two types of data (Table 1).

Sensitivity of indices to spatial resolution

There are great differences in the sensitivity of each of the indices to spatial resolution. LD and LPI are the most robust for both aggregated and actual sensor patterns (Table 1, Table 2, Figure 3). This is consistent across all four zones (Table 1). LPI tends to increase with pixel size in most of the cases because patches near the largest one may merge into it at coarser resolutions. As a consequence, the largest continuous area of a given habitat tends to be overestimated for bigger pixel sizes. An increase in patch size results in lower LD values (Equation (3)). Since both LPI and MPS tend to increase with pixel size, LD decreases at coarser spatial resolutions in most of the cases (Table 1). LD and LPI show quite similar variation trends as a function of class abundance and spatial resolution (Figure 3). Also, the highest sensitivity of both indices to changes in spatial resolutions occurs at class abundance of about 60% (Figure 3). This is a consequence of the high correlation between LD and LPI, with a linear regression between LD and LPI yielding $R^2=0.956$.

NP, EL and MPS are by far the most sensitive indices and thus are not suitable for directly comparing fragmentation of landscape data with different spatial resolutions (Table 1, Table 2, Figure 3). NP and EL decrease and MPS increases rapidly with increasing pixel sizes in the four zones (Table 1, Figure 3). Patch cohesion is considerably sensitive to spatial resolution when class abundance is low (see Figure 3 for class abundance about 10%). But for high class abundance PC is, in general, insensitive to changes in spatial patterns (Gustafson 1998; Saura and Martínez-Millán 2000) or to changes in pixel size (Figure 3, Table 1).

Undesirable behavior of patch cohesion index

NP, MPS, EL, LPI and LD all show lower fragmentation at coarser spatial resolutions (Table 1, Figure 3). This is expected since small patches are "lost" or merge with bigger ones with increasing grain size. However, PC increases for finer spatial resolutions in all four zones (Figure 3, Table 1), indicating higher fragmentation at larger grain sizes. As illustrated in Figure 4, PC increases even if the pattern does not change when mapped at finer resolutions, when the rest of the fragmentation indices remain constant. In fact, an arbitrarily large value of PC, as close to 1 as desired, can be obtained for a given landscape by

Table 1. Values of the fragmentation indices in the four zones for classes 1 (low-NDVI) and 2 (high-NDVI) and three representative cases of class abundance. Table includes the values of the indices corresponding to simultaneously gathered Landsat-TM (30 meters of spatial resolution) and IRS-WiFS (180 meters) images (respectively, "TM-actual" and "WiFS actual") and to Landsat-TM patterns degraded to IRS-WiFS resolution through majority rules ("TM-aggregated", 180 meters of spatial resolution).

			Zone 1			*Zone 2*			*Zone 3*			*Zone 4*		
			Class abundance (%)			*Class abundance (%)*			*Class abundance (%)*			*Class abundance (%)*		
	Class	*Data*	20	50	80	20	50	80	20	50	80	20	50	80
Number of patches	1	TM-actual	32944	21977	27522	36271	31723	11281	45587	40948	14845	34788	46858	21646
		TM-aggregated	1689	1321	893	1261	1117	620	1662	1403	490	1445	2034	487
		WiFS-actual	958	843	716	710	844	519	1012	955	402	1108	2013	788
	2	TM-actual	37084	25664	17299	20786	42683	17334	40395	46840	22145	66513	42288	18272
		TM- aggregated	1675	1052	568	709	1619	575	1275	1565	582	1772	1745	517
		WiFS-actual	1321	616	362	615	966	378	989	1070	415	2818	1434	441
Mean patch size (ha)	1	TM-actual	2.25	8.27	10.36	2.06	5.78	25.46	1.62	4.39	19.08	2.12	3.90	13.76
		TM- aggregated	39.84	136.62	323.46	54.27	166.45	465.34	39.62	129.22	592.15	46.30	88.61	637.22
		WiFS-actual	70.23	198.00	370.32	96.15	193.27	513.35	65.74	172.02	664.04	61.45	81.16	333.45
	2	TM-actual	2.02	6.94	16.53	3.50	4.14	16.46	1.90	3.85	12.92	0.94	4.19	15.66
		TM- aggregated	42.05	169.97	514.06	99.81	107.08	505.81	54.22	113.73	504.19	27.63	102.61	565.54
		WiFS-actual	48.87	264.28	724.92	102.89	172.45	691.64	63.46	154.61	634.17	23.76	115.99	593.24
Edge length (km)	1	TM-actual	17928	18386	20657	17682	25803	11331	22182	29399	17140	18182	32008	24644
		TM- aggregated	3803	4532	4327	3333	5236	2610	4027	5674	3084	3512	7033	3740
		WiFS-actual	2667	3333	3591	2421	3945	2272	3137	4195	2483	3018	6397	5490
	2	TM-actual	20657	18386	17928	11331	25803	17682	17140	29399	22182	24644	32008	18182
		TM- aggregated	4327	4532	3803	2610	5236	3333	3084	5674	4027	3740	7033	3512
		WiFS-actual	3591	3333	2667	2272	3945	2421	2483	4195	3137	5490	6397	3018
Largest patch index	1	TM-actual	8.95	43.66	75.50	10.21	28.28	74.99	4.90	24.16	76.28	5.02	16.63	79.18
		TM- aggregated	9.81	44.67	74.46	11.09	43.83	75.94	6.27	40.97	79.01	3.66	24.63	84.93
		WiFS-actual	11.75	41.76	73.94	13.84	43.02	76.41	7.89	24.54	79.13	6.13	21.12	76.79
	2	TM-actual	3.80	15.47	75.14	9.80	37.28	71.69	6.45	23.31	76.31	1.62	29.03	73.76
		TM- aggregated	5.88	28.35	78.24	14.29	35.90	74.51	7.31	25.83	79.81	3.05	31.64	73.72
		WiFS-actual	8.43	30.12	77.17	12.95	39.07	73.30	6.85	25.92	78.15	4.22	25.57	70.58
Landscape division	1	TM-actual	0.9919	0.8092	0.4300	0.9894	0.9116	0.4375	0.9973	0.9272	0.4181	0.9965	0.9502	0.3730
		TM- aggregated	0.9903	0.8003	0.4448	0.9873	0.8077	0.4232	0.9955	0.8318	0.3757	0.9963	0.9195	0.2787
		WiFS-actual	0.9860	0.8242	0.4520	0.9807	0.8148	0.4161	0.9929	0.9043	0.3738	0.9934	0.9324	0.4103
	2	TM-actual	0.9978	0.9563	0.4353	0.9899	0.8608	0.4854	0.9952	0.9271	0.4177	0.9994	0.9133	0.4553
		TM- aggregated	0.9947	0.9098	0.3878	0.9794	0.8707	0.4435	0.9935	0.9130	0.3630	0.9987	0.8963	0.4550
		WiFS-actual	0.9915	0.9005	0.4045	0.9829	0.8465	0.4616	0.945	0.9084	0.3893	0.9974	0.9231	0.5001
Patch cohesion	1	TM-actual	0.9820	0.9971	0.9968	0.9885	0.9943	0.9973	0.9768	0.9947	0.9986	0.9830	0.9941	0.9982
		TM- aggregated	0.9475	0.9935	0.9905	0.9678	0.9889	0.9930	0.9451	0.9906	0.9966	0.9494	0.9838	0.9961
		WiFS-actual	0.9567	0.9918	0.9893	0.9770	0.9914	0.9929	0.9588	0.9874	0.9965	0.9610	0.9806	0.9953
	2	TM-actual	0.9793	0.9933	0.9976	0.9904	0.9948	0.9968	0.9769	0.9943	0.9984	0.9608	0.9943	0.9986
		TM- aggregated	0.9523	0.9862	0.9947	0.9773	0.9771	0.9952	0.9484	0.9853	0.9973	0.9117	0.9827	0.9961
		WiFS-actual	0.9618	0.9894	0.9959	0.9749	0.9832	0.9955	0.9438	0.9868	0.9970	0.9136	0.9824	0.9963

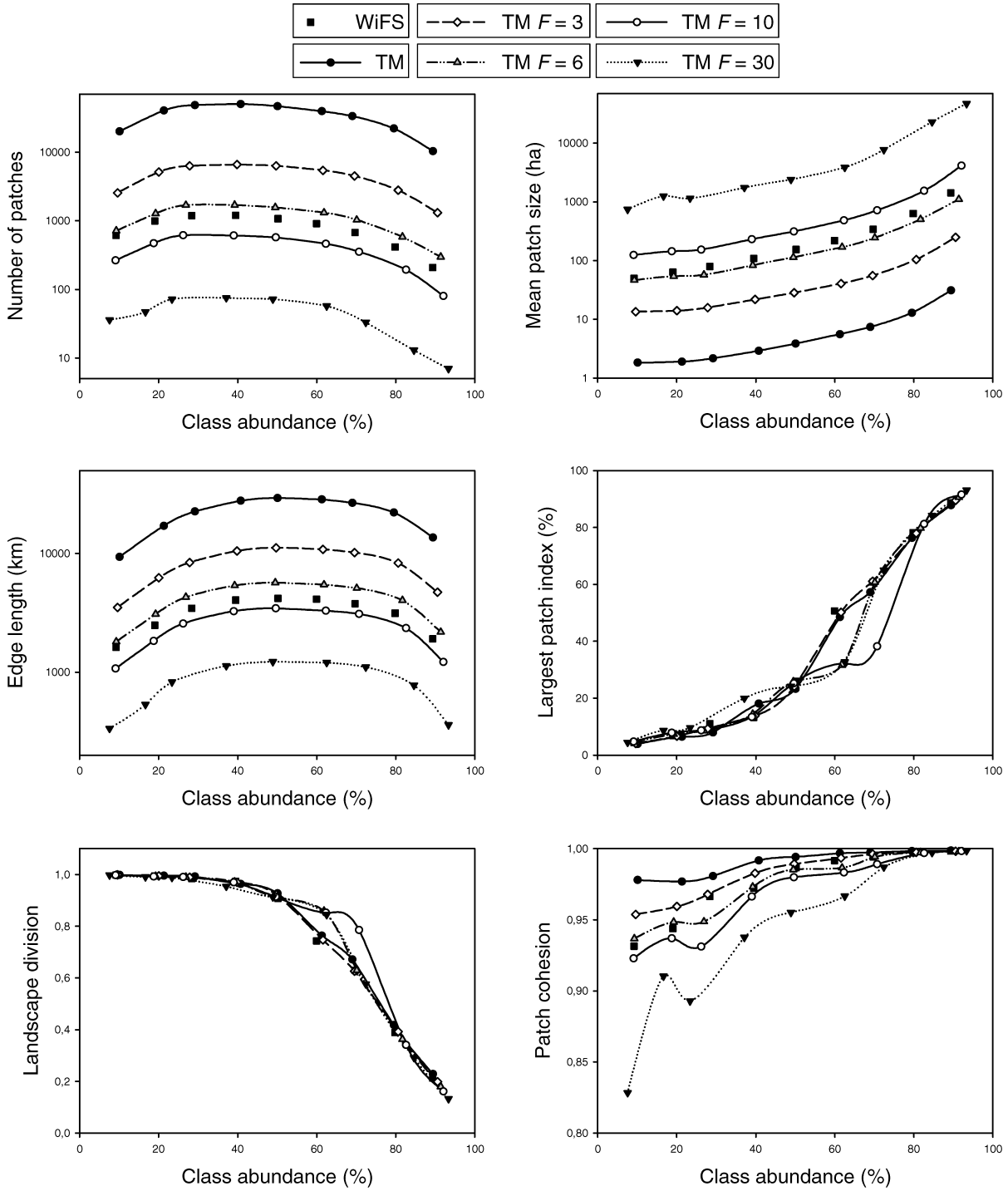

Figure 3. Values of the six fragmentation indices as a function of class abundance for zone 3 and class 2 (high-NDVI). Plots include indices values corresponding to actual TM and WiFS patterns and to TM-patterns aggregated to several coarser resolutions through majority rules. F^2 is the number of original TM-pixels in the aggregating window. Note that the values of number of patches, mean patch size and edge length are shown in logarithmic scale.

Table 2. Mean sensitivity to spatial resolution (S_M) of the six analysed fragmentation indices.

Index	S_M
NP	209.2
MPS (ha)	2880.0
EL (km)	251.5
LPI (%)	12.1
LD	10.6
PC	86.5

simply resampling the pattern at finer spatial resolutions (Saura 2001). This behaviour is a consequence of the dispersal model used by Schumaker (1996) to develop the patch cohesion index, in which dispersal success is defined as the probability that an animal (disperser) is able to find new free territories (not previously occupied by other individuals). Schumaker (1996) defines territories as hexagons of a given size in which at least half of the pixels correspond to habitat suitable for the studied animals (e.g., old growth forests). Territories are then defined on a pixel-basis; the following arguments would not vary if we simply define a territory as a single habitat pixel, and we will consider it so hereafter. For the same number of individuals settled at different points in the landscape, a much larger proportion of total habitat area will be considered as already occupied when pixel size increases (because one individual always occupies the area of one pixel). This makes dispersal success rates decrease, since they depend on the availability of a sufficient number of distinct and non-occupied territories (pixels). Conversely, decreasing pixel size produces a larger number of distinct available territories and a subsequent increase in dispersal success probabilities.

It is possible to correct this undesired behaviour of PC by slightly modifying the expression that Schumaker (1996) provided to calculate PC (Equation (4)). We now consider patch areas and perimeters as the real magnitudes they represent on the ground and adopt the following expression:

$$PC = \left[1 - \frac{\sum_{i=1}^{NP} p_i}{\sum_{i=1}^{NP} p_i \cdot \sqrt{\frac{a_i}{a_{\min}}}} \right] \cdot \left[1 - \frac{1}{\sqrt{\frac{A_T}{a_{\min}}}} \right]^{-1} \quad (6)$$

where p_i and a_i are now expressed as the perimeter and area corresponding on the ground to a certain patch; thus they are no longer defined on a pixel basis. A_T is total landscape area and a_{min} is the area of the smallest patch in a given spatial dataset. Note that if spatial resolution does not vary and a_{min} equals pixel size then Equation (6) simplifies to Equation (4). This modified expression may allow computing PC in vector data, in which there is a certain minimum mapping unit that can be simply made equal to a_{min}. If all patches in the landscape data (either vector or raster) are as small as a_{min} then PC=0. If a single patch fills the landscape then PC=1. Thus the patch cohesion computed according to Equation (6) maintains the original range of variation and interpretation provided by Schumaker (1996). Another possibility is considering a_{min} larger than the smallest patch (excluding patches smaller than a_{min} in the computation of PC, to avoid the possibility of negative values for this index). This will somehow introduce a limitation related to the minimal sizes required for a patch to be considered as a territory suitable for colonization. However, it remains to be tested if the correlations between PC and dispersal success detected by Schumaker (1996) still hold in this case.

The values of PC computed according to Equation (6) are free of the spatial resolution inconsistency described before. PC values now remain constant when spatial resolution varies but the pattern remains invariant (Figure 4). All the patterns in Figure 4 have the same value of a_{min}. As a consequence of this correction, the index now does indicate lower fragmentation at coarser resolutions (Figure 5). This modified version of PC is also considerably more robust to changes in pixel size than the original one: mean sensitivity decreases from 86.5 (Table 2) to 35.5.

Power laws and fragmentation indices

It may be possible to predict the scaling behavior of the most sensitive indices (NP, MPS, EL) and render them comparable across spatial resolutions. Power laws have been used in fractal and earth sciences studies to characterise size distributions of geographical entities and to estimate the scale variations of spatial variables (Feder 1988; Korvin 1992). Several authors have noted that power laws allow predicting the variations of different landscape indices as a function of spatial resolution (Hlavka and Livingston 1997; Frohn 1998; Wu et al. 2000; Saura 2001; Wu et al. 2002):

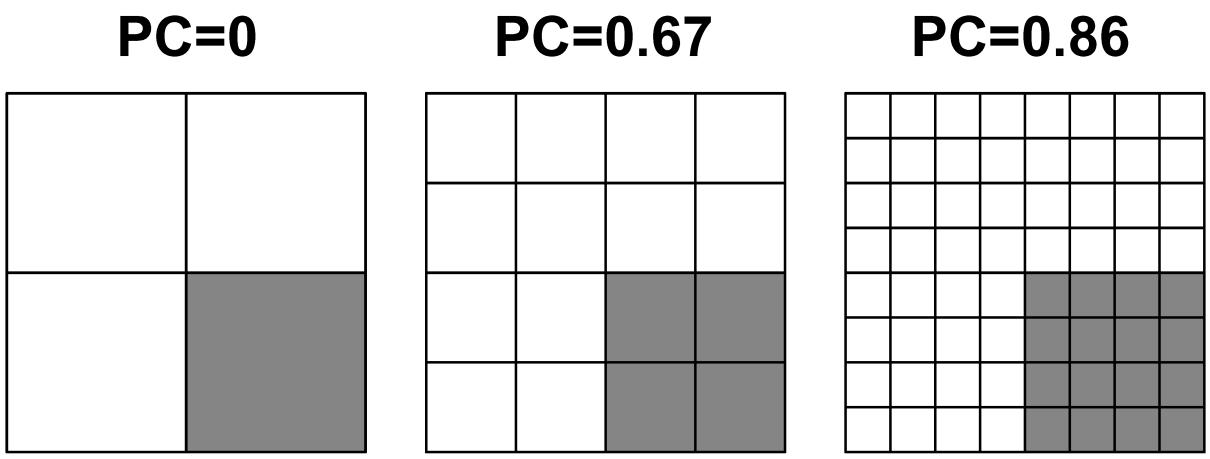

Figure 4. Three patterns in which pixel size has been decreased while maintaining the original spatial configuration. The values of the patch cohesion index (PC) calculated through Equation (4) are shown above each pattern.

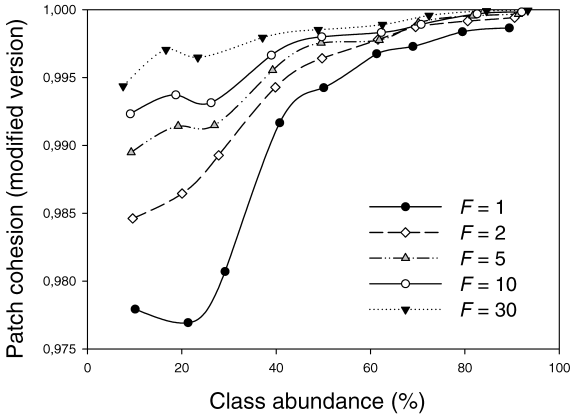

Figure 5. Values of the modified version of the patch cohesion (PC) index (calculated through Equation (6)) as a function of class abundance for zone 3 and class 2 (high-NDVI). PC values corresponding to TM-patterns aggregated to several spatial resolutions through majority rules are included. F^2 is the number of original TM-pixels in the aggregating window. $F=1$ corresponds to actual non-aggregated TM patterns.

$$I(F) = k \cdot F^{-E} \tag{7}$$

or, equivalently,

$$\log(I(F)) = k' - E \cdot \log(F) \tag{8}$$

where I(F) is the value of the index corresponding to the aggregation factor F (F^2 is the number of pixels in the aggregating window). k and k' are constants ($k'=\log k$) and E is the slope of the double-log linear relationship between I and F or, equivalently, the exponent that characterises the power-law ($E > 0$ for indices that decrease at coarser spatial resolutions like NP or EL). Both E and k' were computed as coefficients of the linear least-squares regression given by Equation (8). Equation (8) was fitted to each of the NP and EL values calculated on the Landsat-TM patterns ($F=1$) degraded through majority rules to several spatial resolutions (from $F=1$ to $F=50$). In the case of a perfect fit k' will be equal to $\log(I(1))$, where *I(1)* is the value of the index in the finest spatial resolution data ($F=1$). Estimated MPS values at coarser spatial resolution were obtained through Equation (2) from the values of NP obtained from fitted power laws.

Regressions yielded values of E for the four zones ranging from 1.71 to 2.56 (with mean 1.97) for NP and from 0.85 to 1.19 (with mean 0.97) for EL. In the case of NP, the highest E values were found for class abundance of about 90% and the lowest ones for class abundance of about 30%. In the case of EL, highest E values were obtained both for class abundance of about 90% and 10%, while the lowest ones occurred for the class abundance of 50%. However, class abundance only explained about half of the total variance of E for both indices ($R^2=0.5$ when fitting a second-degree polynomial), and E values did not correlate significantly better with any other of the indices considered in this study. In all the cases we obtained R^2 bigger than 0.96 for NP (over 0.99 in 68 of those 72 cases) and bigger than 0.992 for EL when fitting the power laws to aggregated data (Figure 6). However, logarithms used in Equation (8) tend to underestimate largest residuals and thus may provide

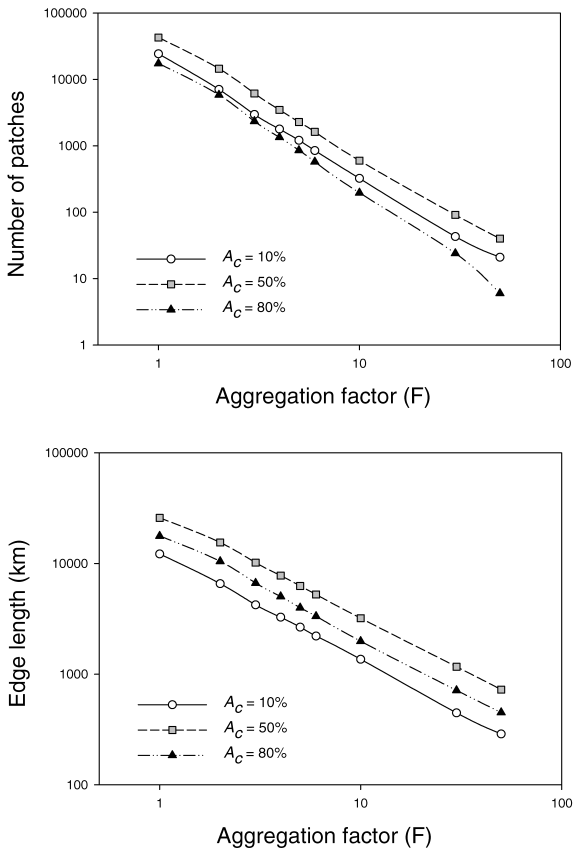

Figure 6. Double-logarithm plot of number of patches and edge length versus spatial resolution (F) for Landsat-TM patterns aggregated through majority rules. Data correspond to zone 2 and class 2 (high-NDVI). Three different cases of class abundance (A_c) are included. F^2 is the number of original TM-pixels in the aggregating window. $F=1$ corresponds to actual non-aggregated TM patterns.

inflated R^2 values. A direct comparison of NP, MPS and EL values computed on aggregated data and obtained from the fitted power-laws (for $F=6$) for the four zones is included in Table 3. We calculated the power-law prediction error as the difference (in absolute value) between the value of the index derived from fitted power law and the one computed in actual aggregated data. The resultant mean relative error for all F values and zones is 9.8% for NP (s.d.= 14.8%), 9.2% for MPS (s.d. = 9.7%), and only 4.5% for EL (s.d. = 4.2%). About 10% of the 72 cases have relative errors higher than 20% for NP and MPS and higher than 10% for EL. Power-laws may be applied not only to NP, MPS and EL, but also to the other less sensitive indices (Wu et al. 2002). For example, Wu et al. (2002) found that the variation of LPI with spatial resolution followed a power function. But in

Table 3. Number of patches, mean patch size and edge length for a spatial resolution of 180 meters corresponding to aggregated patterns and fitted power-laws. Aggregated patterns have been obtained by applying majority rules to Landsat-TM patterns. Table includes indices values for the four zones, classes 1 (low-NDVI) and 2 (high-NDVI) and three representative cases of class abundance.

			Zone 1			*Zone 2*			*Zone 3*			*Zone 4*		
			Class abundance (%)			*Class abundance (%)*			*Class abundance (%)*			*Class abundance (%)*		
	Class	*Data*	20	50	80	20	50	80	20	50	80	20	50	80
Number of patches	1	Aggregated	1689	1321	893	1261	1117	620	1662	1403	490	1445	2034	487
		Power-law	1513	1157	781	1243	1133	601	1621	1374	503	1456	1929	443
	2	Aggregated	1675	1052	568	709	1619	575	1275	1565	582	1772	1745	517
		Power-law	1390	932	524	716	1703	556	1231	1627	554	1831	1597	499
Mean patch size (ha)	1	Aggregated	39.84	136.62	323.46	54.27	166.45	465.34	39.62	129.22	592.15	46.30	88.61	637.22
		Power-law	44.58	156.26	370.37	55.17	164.41	480.85	40.71	132.20	578.24	46.02	93.60	701.39
	2	Aggregated	42.05	169.97	514.06	99.81	107.08	505.81	54.22	113.73	504.19	27.63	102.61	565.54
		Power-law	50.76	192.16	558.78	99.10	102.00	523.81	56.26	109.61	530.60	26.78	112.32	587.59
Edge length (km)	1	Aggregated	3803	4532	4327	3333	5236	2610	4027	5674	3084	3512	7033	3740
		Power-law	3489	4450	3930	3361	5237	2500	4031	5726	2470	3592	6704	3665
	2	Aggregated	4327	4532	3803	2610	5236	3333	3084	5674	4027	3740	7033	3512
		Power-law	3930	4450	3489	2500	5237	3361	2470	5726	4031	3665	6704	3592

our case power-laws provided much poorer predictions for LPI, LD or PC than for NP or EL. For example, for LPI only 30% of the cases had R^2 higher than 0.9 and 28% of the cases had R^2 lower than 0.6.

Discussion

NP, MPS and EL indicate that actual sensor patterns are clearly less fragmented than those aggregated by majority filters. In fact, this is consistent with the data presented in Figure 3 of Benson and MacKenzie (1995): fewer NP and higher MPS in actual AVHRR satellite images than in aggregated data with the same spatial resolution (obtained by applying majority rules to SPOT-HVR images). However, LPI, LD and PC do not show such systematic differences between the two types of data sets. This may be due to the fact that many more small patches, including single isolated pixels, existed in the aggregated images than in the actual WiFS images at the same resolution. NP, MPS and EL are much more sensitive to the amount of small patches in the landscape than LPI, LD and PC (Saura 2002).

Although sensor-specific characteristics could have some impact on the NDVI-patterns (e.g., Teillet et al. 1997), these do not appear sufficient to explain the large differences reported here in terms of pattern fragmentation. These differences may be due mainly to an intrinsic limitation of majority rules for scaling-up landscape configuration. Remote sensors receive the radiation from a certain area of the ground (the instantaneous field of view, IFOV), which is commonly regarded as a perfect squared piece of the Earth's surface. However, this is not true in practice (Cracknell 1998; Huang et al. 2002). First, there is a non-uniform response within the IFOV; objects located near the centre of the IFOV contribute more strongly to the output signal than those farther from it (i.e., sensors present non-linear point spread functions). This is not the case of majority rules, which assign the same weight to all the pixels regardless of their position within the aggregating window. Second, the signal attributed by the sensor to any given pixel is the result of contributions not only from the area strictly corresponding in the ground to that pixel but also from objects located in neighbouring pixels. This means that the way remote sensors acquire the information introduces an additional degree of spatial autocorrelation between pixels (Breaker 1990; Cracknell 1998; Huang et al. 2002). This is added to the intrinsic spatial autocorrelation of landscape patterns. This may explain why simple majority rules are not able to fully replicate the spatial structure in actual sensor patterns. To improve the results provided by simple majority rules it may be necessary to consider the sensor point spread function (PSF). Knowledge of this PSF would allow developing aggregation rules that replicate more closely the spatial configuration of actual sensor patterns. Alternatively, prior to image classification, a deconvolution process could be applied to the images to remove sensor-induced correlation. Several authors have tackled these issues in a remote sensing context (Justice et al. 1989; Breaker 1990; Forster and Best 1994; Cracknell 1998; Huang et al. 2002).

Among the six indices examined in this study, LD and LPI are the most suitable for direct comparison of landscape fragmentation using data with different spatial resolutions (Table 1, Figure 3). LD and LPI have also been shown to be considerably robust to variations in the minimum mapped units of landscape data resulting from an image interpretation process (Saura 2001; Saura 2002). As noted in Saura (2002), LD conveys essentially the same information as the area weighted mean patch size (Li and Archer 1997). The values of these indices are little affected by small patches that are not detected at coarser spatial scales. On the contrary, LD and LPI are not particularly robust to changes in spatial extent (Saura 2001), and other fragmentation indices are more adequate for comparing the fragmentation of patterns with different extents (Saura 2001; Saura and Martínez-Millán 2001; Wu et al. 2002).

Our results show that power-laws were able to predict considerably well the variations of NP and EL with changing pixel size, which is consistent with previous studies (e.g., Frohn 1998; Wu et al. 2000; Wu et al. 2002). However, our results indicate that the exponent of the power law has to be empirically determined by fitting it to the index values computed on aggregated data. In this case, little is gained by fitting a power-law, since the index value at a certain resolution can just be obtained by computing it on aggregated data. However, the interest of such an exponent is that it may also allow obtaining relatively good estimations of the fragmentation index at finer spatial resolutions. This may be the only operational procedure to scale-down fragmentation indices values (i.e., obtaining values of fragmentation indices at finer resolutions based on power-laws developed on coarser resolutions). However, further studies are

needed to know the range of spatial resolution within which such extrapolation provides estimates with a reasonable degree of accuracy. This is part of our ongoing research. It also should be noted that scaling based on power laws fitted to majority-filtered data has at least two sources of error: the statistical error from fitting power-laws to aggregated data and the spatial error due to the differences between aggregated and actual sensor patterns.

Our study compared landscape patterns derived from IRS-WiFS and Landsat-TM images for a central Spain landscape. These results may be verified with other types of landscape data and ranges of spatial resolution different from those considered here. We have focused on six fragmentation indices that are used in the Third Spanish National Forest Inventory, which are only a small set all available fragmentation-related indices (e.g., Hargis et al. 1998, McGarigal and Marks 1995). Also, the indices were computed only at the class-level. Nevertheless, these results may be useful for understanding the behaviour of the same indices at the landscape level.

Acknowledgements

The satellite images used in this study were provided by the Joint Research Centre of the European Commission. Anonymous reviewers made helpful comments on an earlier version of this manuscript.

References

Andrén H. 1994. Effects of habitat fragmentation on birds and mammals in landscapes with different proportions of suitable habitat: a review. Oikos 71: 355–366.

Benson B.J. and MacKenzie M.D. 1995. Effects of sensor spatial resolution on landscape structure parameters. Landscape Ecology 10: 13–120.

Breaker L.C. 1990. Estimating and removing sensor-induced correlation from Advanced Very High Resolution Radiometer satellite data. Journal of Geophysical Research Letters 95: 9701–9711.

Chuvievo E. 1999. Measuring changes in landscape pattern from satellite images: short-term effects of fire on spatial diversity. International Journal of Remote Sensing 20: 2331-2346.

Chuvieco E. 2002. Teledetección ambiental. Ariel, Barcelona, Spain.

Cracknell A.P. 1998. Synergy in remote sensing – what's in a pixel? International Journal of Remote Sensing 19: 2025–2047.

Feder J. 1988. Fractals. Plenium Press, New York, USA.

Forman R.T.T. 1995. Land mosaics: the ecology of landscapes and regions. Cambridge University Press, United Kingdom.

Forster B.C. and Best P. 1994. Estimation of SPOT P-mode point spread function and derivation of a deconvolution filter. ISPRS Journal of Photogrammetric Engineering and Remote Senssing 49: 32-42.

Frohn R.C. 1998. Remote sensing for landscape ecology: new metric indicators for monitoring, modeling and assessment of ecosystems. CRC-Lewis Publishers, Boca Raton, Florida, USA.

Griffiths G.H., Lee J. and Eversham B.C. 2000. Landscape pattern and species richness; regional scale analysis from remote sensing. International Journal of Remote Sensing 21: 2685-2704.

Gustafson E.J. 1998. Quantifying landscape spatial pattern: what is the state of the art? Ecosystems 1: 143–156.

Hansen M.J., Franklin S.E., Woudsma C.G. and Peterson M. 2001. Caribou habitat mapping and fragmentation analysis using Landsat MSS, TM and GIS data in the North Columbia Mountains, British Columbia, Canada. Remote Sensing Environment 77: 50–65.

Hargis C.D., Bissonette J.A. and David J.L. 1998. The behavior of landscape metrics commonly used in the study of habitat fragmentation. Landscape Ecology 13: 167–186.

Hlavka C.A. and Livingston G.P. 1997. Statistical models of fragmented land cover and the effect of coarse spatial resolution on the estimation of area with satellite sensor imagery. International Journal of Remote Sensing 18: 2253-2259.

Huang C., Townshend J.R.G., Liang S. Kalluri S.N.V. and DeFries R.S. 2002. Impact of sensor's point spread function on land cover characterization: assessment and deconvolution. Remote Sensing Environment 80: 203-212.

Imbernon J. and Branthomme A. 2001. Characterization of landscape patterns of deforestation in tropical rain forests. International Journal of Remote Sensing 22: 1753-1765.

Iverson L.R. 1988. Land-use changes in Illinois, USA: The influence of landscape attributes on current and historic land use. Landscape Ecology 2: 45-61.

Jaeger J.A.G. 2000. Landscape division, splitting index, and effective mesh size: new measures of landscape fragmentation. Landscape Ecology 15: 115-130.

Jelinski D.E. and Wu J. 1996. The modifiable areal unit problem and their implications for landscape ecology. Landscape Ecology 11: 129-140.

Justice C.O., Markham B.L., Townshend J.R.G. and Kennard R.L. 1989. Spatial degradation of satellite data. International Journal of Remote Senssing 10: 1539-1561.

Korvin G. 1992. Fractal models in the earth sciences. Elsevier Science Publishers, Amsterdam, The Netherlands.

Li B. and Archer S. 1997. Weighted mean patch size: a robust index for quantifying landscape structure. Ecology Modelling 102: 353–361.

Li H., Franklin J.F., Swanson F.J. and Spies T.A. 1993. Developing alternative forest cutting patterns: a simulation approach. Landscape Ecology 8: 63-75.

Luque S.L., Lathrop R.G. and Bognar J.A. 1994. Temporal and spatial changes in an area of the New Jersey Pine Barrens landscape. Landscape Ecology 9: 287–300.

Luque S.S. 2000. The challenge to manage the biological integrity of nature reserves: a landscape ecology perspective. International Journal of Remote Sensing 21: 2613-1643.

Ministerio de Medio Ambiente 2002. Tercer Inventario Forestal Nacional. Dirección General de Conservación de la Naturaleza. Madrid, Spain.

Myneni R.B., Hall F.G., Sellers P.J. and Marshack A.L. 1995. The interpretation of spectral vegetation indices. IEEE Trans. Geoscience and Remote Sensing 33: 481–486.

McGarigal K. and Marks B.J. 1995. Fragstats: spatial pattern analysis program for quantifying landscape structure. USDA Forest Service General Technical Report PNW-GTR-351. Corvallis, Oregon, USA.

NRSA 1995. IRS-1C data user's handbook. Indian National Remote Sensing Society. Hyderabad, India.

O'Neill R.V., Hunsaker C.T., Timmins S.P., Jackson B.L., Jones K.B., Riitters K.H. and Wickham J.D. 1996. Scale problems in reporting landscape pattern at the regional level. Landscape Ecology 11: 169–180.

Openshaw S. 1984. The Modifiable Areal Unit Problem. Geo Books, Norwich, UK.

Sachs D.L., Sollins P. and Cohen W.B. 1998. Detecting landscape changes in the interior of British Columbia from 1975 to 1992 using satellite imagery. Canadian Journal of Forest Research 28: 23–36.

Saura S. 2001. Influencia de la escala en la configuración del paisaje: estudio mediante un nuevo método de simulación espacial, imágenes de satélite y cartografías temáticas. Ph. D. Thesis, Universidad Politécnica de Madrid, Spain.

Saura S. 2002. Effects of minimum mapping unit on land cover data spatial configuration and composition. International Journal of Remote Sensing 23: 4853-4880.

Saura S. and Martínez-Millán J. 2000. Landscape patterns simulation with a modified random clusters method. Landscape Ecology 15: 661–678.

Saura S. and Martínez-Millán J. 2001. Sensitivity of landscape pattern metrics to map spatial extent. Photogrammatic Engeneering and Remote Sensing 67: 1027-1036.

Schumaker N.H. 1996. Using landscape indices to predict habitat connectivity. Ecology 77: 1210–1225.

Teillet P.M., Staenz K. and Williams D.J. 1997. Effects of spectral, spatial and radiometric characteristics on remote sensing vegetation indices of forested regions. Remote Sensing Environment 61: 139–149.

Tischendorf L. 2001. Can landscape indices predict ecological processes consistently? Landscape Ecology 16: 235–254.

Turner M.G. and Ruscher C.L. 1988. Changes in landscape patterns in Georgia, USA. Landscape Ecology 1: 241–251.

Turner M.G., O'Neill R.V., Gardner R.H. and Milne B.T. 1989a. Effects of changing spatial scale on the analysis of landscape pattern. Landscape Ecology 3: 153–162.

Turner M.G., Costanza R. and Sklar F.H. 1989b. Methods to evaluate the performance of spatial simulation models. Ecology Modelling 48: 1–18.

Wickham J.D. and Riitters K.H. 1995. Sensitivity of landscape metrics to pixel size. International Journal of Remote Sensing 16: 3585–3594.

Wu J., Jelinski D.E., Luck M. and Tueller P.T. 2000. Multiscale analysis of landscape heterogeneity: scale variance and pattern metrics. Geographical Information Science 6: 6–19.

Wu J., Shen W., Sun W. and Tueller P.T. 2002. Empirical patterns of the effects of changing scale on landscape metrics. Landscape Ecology 17: 761-782.